Environment Protection Engineering

Vol. 16 1990 No. 1

MICHAŁ GŁOMBA*

THE SCRUBBING OF COMBUSTION GAS TAKEN OFF AN IRON ORE SINTER BELT IN A SPRAY SCRUBBER WITH THE CROSS-FLOW OF PHASES

The design of a spray scrubber with the cross-flow of phases that has been tested for the hydraulics of flow of the gaseous phase and the effectiveness of scrubbing depending on the linear velocity of the jet of combustion gas produced during the sintering of iron ore and the size of the jet of liquid atomized in the scrubber is presented. Relationships useful for determining the resistance of flow of the gaseous phase in the scrubber and the fractional and overall effectiveness of the scrubbing of the combustion gas produced in the process of iron ore sintering are given.

SYMBOLS

A – longer side of scrubber in projection, m,
A_K – phase contact surface developed on drops of liquid, m^2,
a – surface of drops per unit of scrubber's volume, m^2/m^3,
B – shorter side of scrubber in projection, m,
C – concentration of gas particles in combustion gas, g/m^3 (in normal conditions),
D_h – equivalent diameter of scrubber's flow section, m,
d_1, d_2 – diameters of scrubber's inlet and outlet connector pipes, mm,
d_a – dust particles diameter, μm (m),
d_s – average (Sauter) diameter of drops, m (μm),
H_K – scrubber's active height, m,
h_k – distance between partitions in working part of scrubber, m,
l – length of path of combustion gas flow in scrubber, m,
l_i – length of partition, m,
l_k – length of interphase contact path, m,
l_s – distance between partitions in separation part of scrubber, m,
N_t – number of transfer units,

* Institute of Environment Protection Engineering, Technical University of Wrocław, pl. Grunwaldzki 9, 50-377 Wrocław, Poland.

n_0 – number of atomizers in inlet space of scrubber,
n_i – number of atomizers in interpartition space,
n – total numberof atomizers,
P_t – power supplied to scrubber, kJ/1000 m^3,
P_L – liquid pressure before atomizers, Pa,
Δp – gaseous phase pressure losses in scrubber, Pa,
U_G – linear velocity of combustion gas in scrubber, m^3/h,
$\dot{V}_G$ – volumetric jet of combustion gas in scrubber (in normal conditions), m^3/h,
$\dot{V}_L$ – volumetric jet of atomized liquid, m^3/h,
α – coefficient,
β – coefficient,
η – overall effectiveness of combustion gas scrubbing,
η_f – fractional effectiveness of combustion gas scrubbing,
η_i – effectiveness of inertial precipitation of dust particles on drop of liquid,
λ – drag coefficient of combustion gas flow in scrubber,
ρ_G – density of combustion gas in normal conditions, kg/m^3.

1. INTRODUCTION

One of the ways in which iron ore is dressed for the blast furnace is sinterning. It consists in the agglomeration of fine-grained ores and powdery concentrates, with ground flux and fly-ash added, into lumps suitable for charging into the blast furnace. A Dwight–Lloyd belt machine is usually used for this purpose. A general diagram of such a sintering plant is shown in fig. 1. The sintering plant consists of sinter belt *1* stretched over two drums *2* and moving on rollers. Before the sinter mix is fed, the belt is covered with cold return sinter carried by belt conveyor *10* to feeder

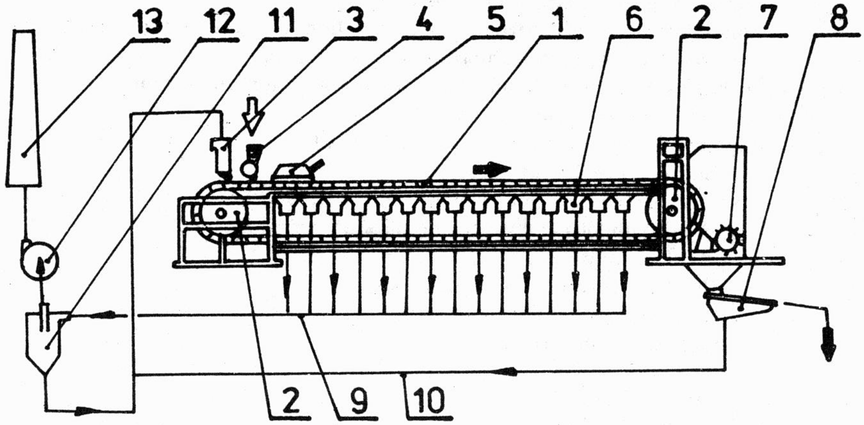

Fig. 1. A diagram of the iron ore sintering plant

3, in order to protect the belt against overheating. The mix is fed onto it through feeder *4*. Further on, there is gas burner *5* that heats the charge up to the ignition temperature of loke. Fly-ash is burnt in the presence of oxygen sucked in with air through the charge belt as it moves over suction chamber *6*. At the other end of the belt, i.e., where it changes its direction of movement, the sintered material falls down to breaker *7* and then the crushed sinter is screened by sieves *8*. Screenings of below 5 mm grain size are returned to feeder *3* and lumpy sinter is fed onto the cooler belt where it is cooled down to the temperature of about 338 K. The ready sifted sinter of 5–50 mm size is transported to blast furnace bunkers.

As the hot combustion gas passes through the sinter mix bed, it gives up its heat and is cooled down from the temperature ranging from 1673 K to 373–573 K. Most of gas and dust is sucked off from the end part of the belt, whereas the amount of dust in the first half of the belt is small. The average concentration of dust in the gas drawn off from chambers *6* is about 10 g/m^3 and the amount of dust carried by the gas constitutes about 3–4% of the sinter production [1], [2]. The amount of dust raised from the belt is 11 kg per 1 ton of sinter. The size analysis of the dust contained in the gas according to [2] is presented in table 1 while its chemical constitution is shown in table 2.

Table 1

Size analysis of the dust in the combustion gas coming from the conveyor belt

Grain size d_a (μm)	1.0	1.5	2.0	5.0	10.0	15	20	30	40	60	70	80	100	150	200
Mass fraction (%)	2.0	3.5	5.0	12.0	20.0	24.0	26.0	32.0	40.0	55.0	59.0	65.0	70.0	85.0	97.0

Table 2

Chemical constitution of the dust produced during the sintering of iron ore

Constituent	Mass fraction (%)
Sintering loss	25.5
Fe_2O_4	40.8
SiO_2	5.4
Al_2O_3	0.8
CaO	5.4
MgO	1.1
Alkalies	8.3
C	3.8
F	0.5
Zn	0.1
Other	8.3

The dusty gas is transported through duct *9*, to dust collection plants *11*, where it is cleaned and then via fan *12* and chimney *13* it is emitted into the atmosphere. Since cyclones, multicyclones or electro-filters may serve as dust collection plants, the emission figures will differ depending on the dust collector. The efficiency of dust extraction in cyclones is 70%, in multicyclones 85% and in electro-filters about 99%. Therefore, in the first two cases a second stage of dust extraction is needed.

The process of ore sintering produces not only dust but gas pollutants as well. The amounts of the particular gaseous constituents in the combustion gas depend on the composition of the mix, the amount of gas and the volume of sinter production. The chemical constitution according to [1] is given in table 3. In order to lower the pollution of air by carbon monoxide, after-burning with gas burners is used whereby its emission can be reduced from 40 kg/t sinter to 2 kg/t sinter.

Table 3

Average chemical constitution of the combustion gas

Constituent	Volume fraction (%)
O_2	10–20
CO_2	4–10
CO	0–6
SO_2	0–0.4
N_2	86–64

The SO_2 content in the combustion gas depends on the sulfur content in the sinter's components and in the fuel gas. The amount of SO_2 produced in an ore sintering plant may reach 1.5 kg/t sinter. In old but still active ore sintering plants SO_2 is not removed from the combustion gas and this together with the dustiness of the gas, despite the dust extraction carried on in cyclones or multicyclones, requires an installation that would reduce substantially both dust and SO_2. Due to its simple design and the relatively low energy requirements, a spray scrubber with the cross-flow of phases [3] can fulfil this task. The scrubber was tested for real gases in one of the iron ore sintering plants. The size analysis of the dust contained in the combustion gas between the multicyclone and the scrubber is given in table 4.

Table 4

Size analysis of the dust in the combustion gas before the scrubber

Grain size d_a (μm)	2	4	6	8	10	20	30	40
Mass fraction (%)	10	18	29	41	55	78	87	96

2. THE SCRUBBER'S DESIGN

The spray scrubber with the cross-flow of phases was designed for the following loads:

the gaseous phase: up to 12,000 m^3/h in normal conditions,

the liquid phase: up to 43 m^3/h.

The scrubber's diagram is shown in fig. 2. Its operation consists in the cross contacting of the gaseous phase with the liquid phase and the simultaneous development of a phase contact surface on a polydispersion collection of drops produced by the spraying of liquid by means of hydraulic atomizers. The jet of gas in contact with liquid drops changes its direction of flow several times whereby it is mixed more throughly and the mass and heat exchange process has a higher driving moduls. The characteristic dimensions of the scrubber are given in table 5. Centrifugal atomizers of the "Klimator" type of 4.3 mm outlet diameter were used in

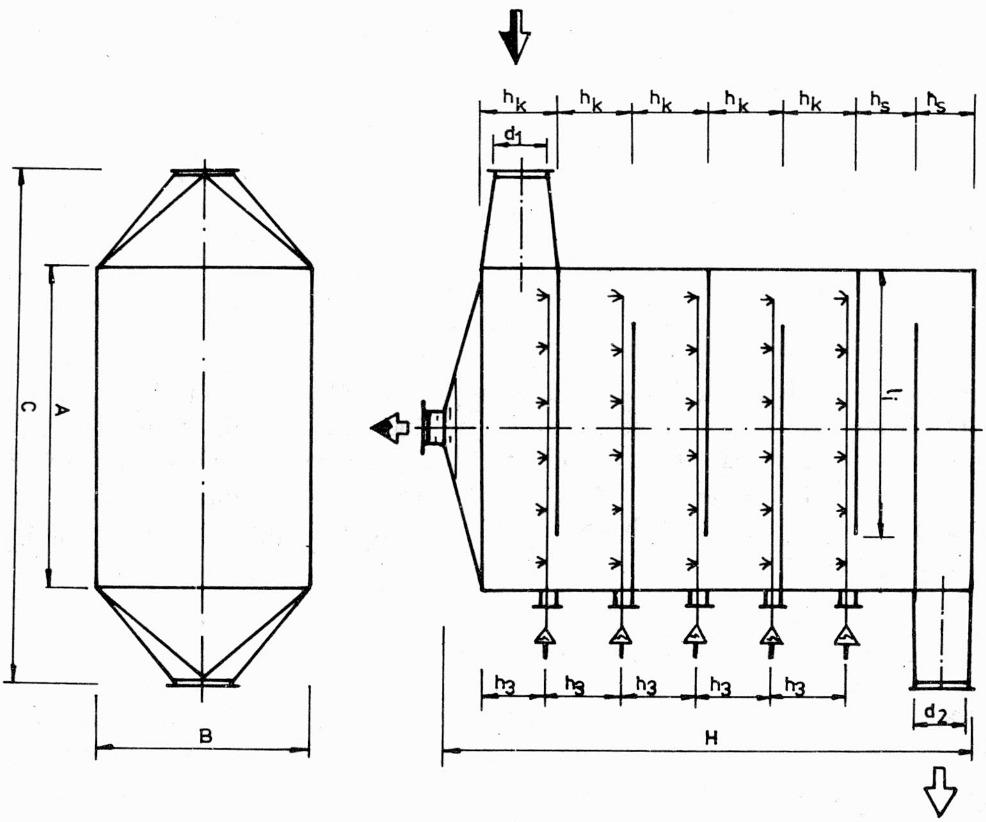

Fig. 2. A diagram of the spray scrubber with the cross-flow of phases

the tests. The hydrodynamic parameters of liquid atomization by "Klimator" atomizers are given in [4]. The change in the direction of flow of the cleaned combustion gas and the breaking of the film of liquid flowing down from a higher to a lower partition have a favourable effect on the inertial precipitation of dust particles on liquid drops.

Table 5

Characteristic dimensions of the scrubber

Functional dimension	Unit of measure	Numerical value
Diameter of gas inlet connector pipe, d_1	mm	500
Diameter of gas outlet connector pipe, d_2	mm	500
Dimension of scrubber longer side, A	m	3.0
Dimension of scrubber shorter side, B	m	2.0
Height between partitions in working part of scrubber, h_k	m	0.7
Height between partition in separation part of scrubber, l_s	m	0.5
Active height of scrubber, $H_k = 5h_k$	m	3.5
Length of gas flow path in scrubber, l	m	21.9
Length of interfacial contact, l_k	m	15.9
Length of partition, l_i	m	2.5
Number of atomizers in inflet space, n_0	pieces	44
Number of atomizers in space between adjecent partitions, n_i	pieces	24
Total number of atomizers, n	pieces	140

3. TESTING

The spray-scrubber with the cross-flow of phases and the given above liquid and gaseous phase loads was subjected to tests which were to determine the flow hydraulics of the gaseous phase, the effect of the scrubbing of the gas coming from the sinter belt and the kinetics of SO_2 absorption in NaOH solution according to the dialkaline method [5], [6]. In this paper, the presentation of results is limited to the first two problems.

4. THE FLOW HYDRAULICS OF THE GASEOUS PHASE

The drop of gas pressure in the scrubber was determined by measuring static pressures at its inlet and outlet at linear gas velocities $U_G = 0.5$, 1.0, 1.5, 2.0, 2.5, 3.0 m/s and rates of the atomized jet of liquid $\dot{V}_C = 0.0$, 10.0, 20.0, 30.0, 45.0 m^3/h. The results are presented in the form of diagrams showing the relationship between the pressure drop and the flow velocity (fig. 3) and the relationship between the gas flow drag coefficient and the surface of drops per unit of the scrubber's volume

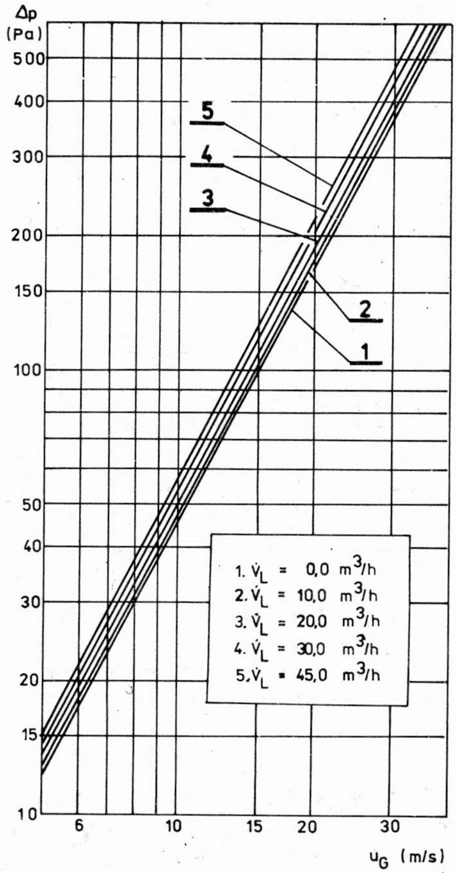

Fig. 3. The drop of combustion gas pressure in the scrubber as a function of the linear velocity

(fig. 4). The results of the studies of the gas pressure drop in the scrubber with the cross-flow of phases are also expressed by the equation

$$\Delta p_G = \lambda \frac{l}{D_h} \cdot \frac{U_G^2 \rho_G}{2}.$$

The diagram in fig. 4 shows the values of the gas flow drag coefficient. It can be seen that the spraying of the scrubber has an insignificant effect on the pressure drop of the flowing gas. Within the range 0–45 m^3/h of the atomized jet of liquid which corresponds to 0–3 m^2/m^3 of the surface of drops per unit of the scrubber's volume, the resistance of flow of the gaseous phase increases by 21.5%. The surface of drops per unit of the scrubber's volume is given by the relationship

$$a = \frac{A_k}{V_{skr}} = \frac{6\,\dot{V}_L\,C\,h_K}{U_K\,d_s\,A\,B\,H_K\,3600}.$$

In this case, coefficient $C = 0.8$ (it takes into account this part of the height between

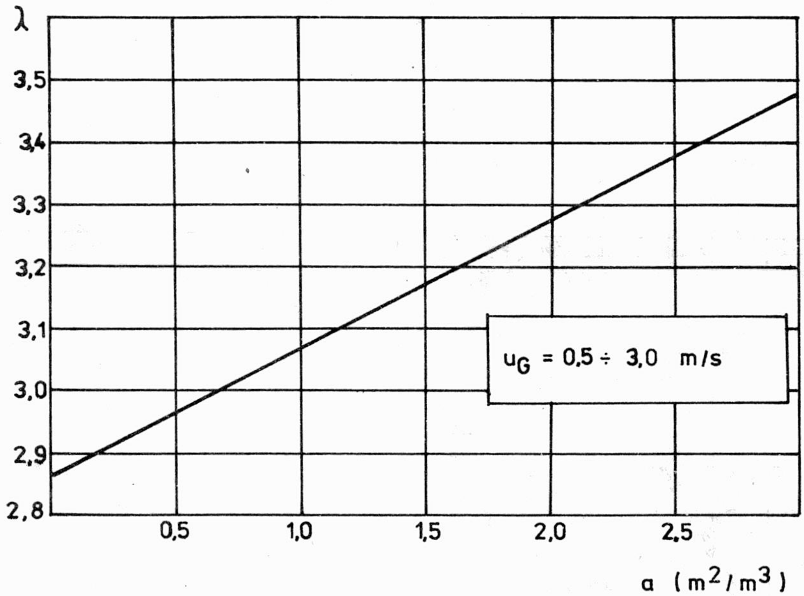

Fig. 4. The relationship between the drag coefficient of combustion gas flow and the surface of drops per a unit of the scrubber's volume

partitions where the atomization of the liquid occurs whereby the scrubber's volume taken up by the liquid collectors together with the atomizers can be left out).

5. THE SCRUBBING OF THE COMBUSTION GAS

The effect of the combustion gas scrubbing was determined for scrubber gas linear velocity U_G from 0.5 to 3.0 m/s and the efficiency of scrubbing was established for rates of the atomized jet of liquid $\dot{V}_L = 20, 30, 45$ m^3/h. Surface of drops per unit of the scrubber's volume $a = 1.4, 2.1, 3.1$ m^2/m^3 correspondend to the above jets of liquid. Surface of phase contact $A_K = 29.3, 43.9, 65.9$ m^2 corresponded to the latter figures.

The effectiveness of scrubbing as a function of the linear velocity of the gas in the flow section of the scrubber is shown in a diagram form in fig. 5. For gas velocities over 1.0 m/s, the efficiency of scrubbing depends a lot on the amount of the atomized liquid, particularly at $\dot{V}_L < 30$ m^3/h. This was confirmed by studies of the dependence of the scrubbing efficiency on the size of the jet of the atomized liquid conducted for gas linear velocities U_G: 1.0, 2.0, 3.0 m/s (fig. 6).

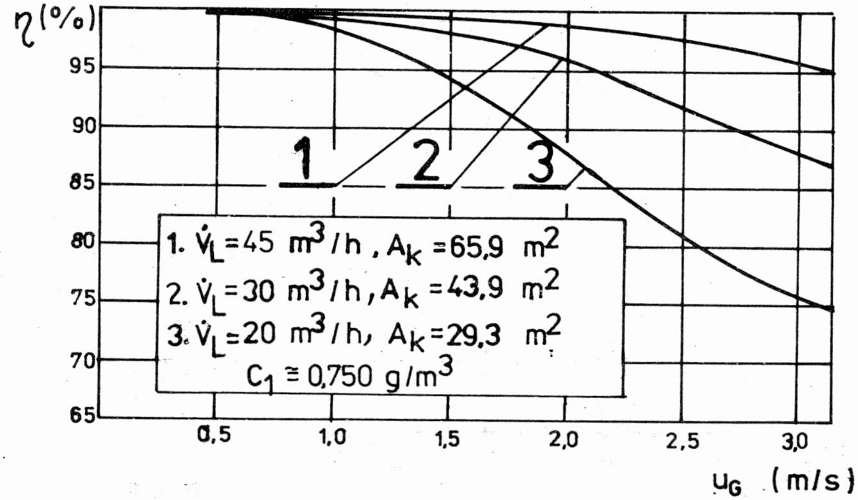

Fig. 5. The relationship between the effectiveness of scrubbing and the linear velocity of combustion gas in the scrubber

The overall effectiveness of the combustion gas scrubbing in a spray scrubber with the cross-flow of phases can be described with great accuracy by the following equation determined on the basis of the tests

$$\eta = 1 - \exp\left(-\frac{0.88\, A_K}{4\, \dot{V}_G\, 3600}\right).$$

It follows from the above that the overall effectiveness of scrubbing is directly proportional to the interfacial surface developed in the scrubber on drops of atomized liquid and inversely proportional to the volumetric jet of the combustion gas cleaned there.

The results of the testing of the fractional efficiency of the combustion gas scrubbing at volumetric jet of atomized liquid $\dot{V}_L = 20$, 30, 40 m^3/h and linear velocity of the combustion gas in the scrubber $U_G = 3$ m/s are of particular interest. The fractional efficiency of the gas scrubbing is shown in fig. 7. It follows from the curves that as the diameter of dust particles falls below 5 μm, the fractional efficiency drops abruptly, whereas for particles of above 10 μm diameter, it is very stable. On the basis of the tests, the fractional efficiency of the combustion gas scrubbing in the spray-scrubber with the cross-flow of phases was described by the equation

$$\eta_f = 1 - \exp\left(-\frac{3\, \dot{V}_L\, C\, h_K}{2\, \dot{V}_G\, d_s}\, \eta_i\right).$$

Coefficient C reflects the incomplete utilization of the inter-partition space for liquid drops formation due to the mounting under the partitions of liquid collectors with the sprayers' nozzles pointing downwards. For the tested scrubber, $C = 0.8$.

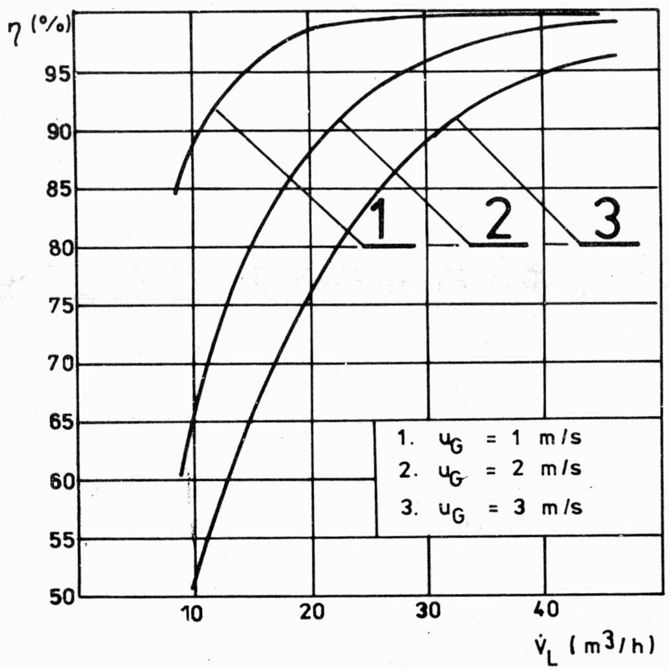

Fig. 6. The relationship between the effectiveness of scrubbing and the size of the jet of the atomized liquid

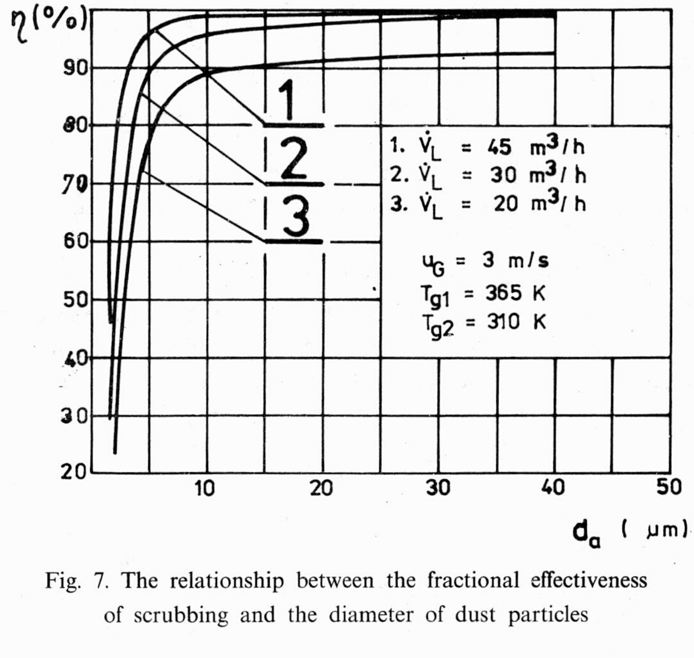

Fig. 7. The relationship between the fractional effectiveness of scrubbing and the diameter of dust particles

Effectiveness of the inertial precipitation of dust particles on a drop of liquid η_i is a function of the Stokes number and it should be determined using the relationships given in references [7] and [8].

6. THE DEPENDENCE OF SCRUBBING EFFECTIVENESS ON THE ENERGY SUPPLIED TO THE SCRUBBER

Studies of wet dust collectors' operation show that for given dust, the effectiveness of the collector's operation is a function of the supplied energy, independent of the kind, the type or the geometric dimension. SEMRAU [9] called the energy per unit of the cleaned gas *contacting power*. According to the adopted hypothesis, scrubbers of any design, where separation of particles from the jet of gas is a result of

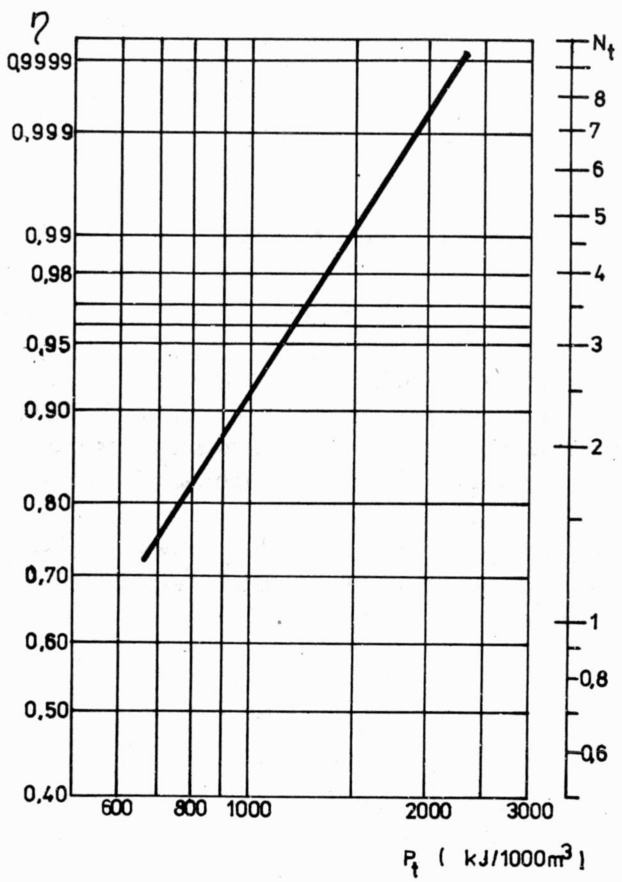

Fig. 8. The relationship between the effectiveness of scrubbing and the energy consumption

the action of intertial forces, having the same contacting power will have the same scrubbing effectiveness. The relationship between scrubbing effectiveness and contacting power for different aerosol systems and wet dust collectors can be found in references [9], [10]. However, there are no available literature data on the aerosol system that is produced during the sintering of iron ore. Such a relationship obtained from the test is shown as a diagram in fig. 8. The diagram can be interpreted mathematically as

$$\eta = 1 - \exp(-\alpha P_t^{\beta}),$$

where coefficients α and β were determined experimentally ($\alpha = 5.38 \cdot 10^{-5}$, $\beta = 1.558$).They represent the grain characteristics of the dust and its kind. At scrubbing effectiveness over 98%, the changes in effectiveness due to changed operational parameters of the dust collector are weakly marked and therefore, when evaluating its operation, it is better to use the number of units of transfer defined as

$$N_t = \ln\left(\frac{1}{1-\eta}\right).$$

From the two above equations it follows that

$$N_t = \alpha P_t^{\beta}.$$

The total energy supplied to the scrubber was determined from the relationship

$$P_t = \Delta p_G + \frac{\dot{V}_L}{\dot{V}_G} p_L.$$

The value of coefficient $\beta < 1$ indicates that the mass fraction of sub-microscopic particles is large and not only the inertial mechanism but also the diffusion mechanism and the condensation of steam that increases the mass of dust particles and the forces of thermo- and diffusionphoresis influence the effectiveness of scrubbing.

Curve $\eta = f(P_t)$ in fig. 8 shows that high effectiveness of sinter gas scrubbing in a scrubber with the cross-flow of phases can be achieved at relatively low energy consumption.

7. CONCLUSIONS

The conducted tests of the effectiveness of the scrubbing of combustion gas, produced during the sintering of iron ore, in a spray scrubber with the cross-flow of phases proved it to be a suitable apparatus for the second stage of the extraction of dust from the gas.

At appropriate ratio $\frac{\dot{V}_L}{\dot{V}_G}$ (about 3.75 in normal conditions) and at linear velocity of the gas in the scrubber $U_G = 3.0$ m/s and diameter of drops $d_s \leqslant 550$ μm, effectiveness of scrubbing $\eta \geqslant 0.96$ is obtained.

The high effectiveness of scrubbing is achieved at relatively low energy consumption (at $P_t \geqslant 1500$ kJ/1000 m^3, $\eta \geqslant 0.99$).

Besides the inertial mechanism, the diffusion mechanism and the condensation of water vapour contained in the combustion gas influence the effectiveness of scrubbing.

Because of the scale of the tested scrubber, the obtained correlation can be applied with great likelihood to its enlarged versions.

REFERENCES

[1] JĘDRZEJOWSKI J., *Procesy przemysłowe a zanieczyszczenie środowiska. Przemysł hutniczy i cementowy* (in Polish), PWN, Warszawa 1987.

[2] JUDA J., CHRÒŚCIEL S., *Ochrona powietrza atmosferycznego* (in Polish), WNT, Warszawa 1974.

[3] Patent PRL, No. 101910.

[4] GŁOMBA M., *Parametry rozpylania cieczy dyszą kątową typu "Klimator"* (in Polish), Ochr. Pow., No. 6 (1983), pp. 149–152.

[5] Patent PRL, No. 123036.

[6] GOSTOMCZYK M., GŁOMBA M., *Technologia odsiarczania spalin. Charakterystyka procesu i założenia projektowe* (in Polish), Raport serii SPR No. 6/82 (1982).

[7] WARYCH J., *Oczyszczanie przemysłowych gazów odlotowych* (in Polish), WNT, Warszawa 1988.

[8] KNETTIG P., BEECKMANS I. M., J. Aerosol Sci., No. 5 (1974), p. 235.

[9] SEMRAU K. T., Chem. Eng., No. (1977), p. 87.

[10] SEMRAU K. T., Staub., No. 22 (1962), p. 184.

ODPYLANIE W SKRUBERZE NATRYSKOWYM O KRZYŻOWYM PRZEPŁYWIE FAZ SPALIN UJMOWANYCH Z TAŚMY SPIEKALNICZEJ RUDY ŻELAZA

Przedstawiono konstrukcję skrubera natryskowego o krzyżowym przepływie faz. W skruberze tym zbadano hydraulikę przepływu fazy gazowej i skuteczność odpylania spalin powstających podczas spiekania rudy żelaza. Badane procesy zależą od prędkości liniowej strumienia spalin i wielkości strumienia rozpylanej w skruberze cieczy.

Podano korelacje przydatne do określania oporów przepływu fazy gazowej w skruberze oraz frakcyjnej i całkowitej skuteczności odpylania spalin.

ОБЕСПЫЛИВАНИЕ В НАБРЫЗГИВАЮЩЕМ СКРУББЕРЕ КРЕСТООБРАЗНОГО ТЕЧЕНИЯ ФАЗ ДЫМОВЫХ ГАЗОВ, ЗАХВАТЫВАЕМЫХ С АГЛОМЕРАЦИОННОЙ ЛЕНТЫ ЖЕЛЕЗНОЙ РУДЫ

Представлена конструкция набрызгивающего скруббера крестообразного течения фаз. В этом скруббере испытаны гидравлика течения газовой фазы и эффективность обеспыления дымовых газов, образующихся во время агломерирования железной руды. Исследуемые процессы зависят от линейной скорости потока дымовых газов и размера потока набрызгиваемой в скруббере жидкости.

Даны зависимости, пригодные для определения сопротивлений течения газовой фазы в скруббере, а также фракционной и полной эффективностей обеспыления дымовых газов.